JREE: Vol. 10, No. 4, (Autumn 2023) 44-58

Journal of Renewable Energy and Environment

Journal Homepage: www.jree.ir

Materials and Energy Research Center

MERC

Research Article

A Novel Approach to Fast Determining the Maximum Power Point Based on Photovoltaic Panel's Datasheet

Sameer Hanna Khader[a]*, Abdel-Karim Khalid Daud[a]

[a] *Department of Electrical Engineering, Faculty of Engineering, Palestine Polytechnic University, P. O. Box: 198, Hebron, Palestine.*

PAPER INFO

Paper history:
Received: 13 September 2022
Revised: 18 January 2023
Accepted: 31 January 2023

Keywords:

Buck-Boost Converter,
Traditional SEPIC Converter,
Modified SEPIC Converter,
MPPT

ABSTRACT

This study proposes a novel approach to fast and direct determination of the Maximum Power Point (MPP) at any value of solar irradiation and cell temperature, without applying further mathematical processing to operate at that point. The current approach aims to reduce algorithm complexity, time consumption during the iteration, and oscillation to reach the point at which the panel generates maximum possible power. For avoiding or eliminating these drawbacks, the chopper duty cycle (D) at which the panel-generated power should be the maximum is determined using the panel datasheet with respect to voltage and power at different irradiation rates (G). Mathematical equations are derived for MPP voltage and power at any value of solar irradiation using the manufacturer Photovoltaic (PV) specification. The simulation results obtained by MATLAB/SIMULINK platform showed that the power had a linear change, while the voltage had a nonlinear one with narrow variations. The yield duty cycle controls the Modified Single Ended Primary Converter (MSEPIC) that regulates the load voltage through a wide range below and above the rated panel voltage. The simulation results showed the fast response of chopper operation with a negligible starting time required by the MPPT algorithm, no duty cycle oscillation, and shorter iteration time. Furthermore, the conducted approach is validated based on the data published in a reputed journal, and the obtained results gave rise to new aspects that helped reduce dependency on conventional MPPT algorithms and, consequently, enhance the system response, efficiency and cost reduction.

https://doi.org/10.30501/jree.2023.361697.1450

1. INTRODUCTION

Renewable energy sources enjoyed many different applications in three decades ago, mainly in photovoltaic and solar systems, wind energy systems, biogenertors, and other non-conventional sources. The great tendency for the growth of these sources is pushed ahead due to instability of international markets for fossil oils, conducted efforts for saving and protecting the environment, and high cost of traditional oil and gas as mentioned (Martini et al, 2015) and (Mahmoud Y. et al., 2012) in their studies. In addition, these sources suffer greatly from expected depletion in the near future. Consequently, intensive research is encouraged on the development of advanced renewable sources such as photovoltaic (PV) generators. (Khader et al, 2021) described a Photovoltaic generator consists of solar panels, DC chopper, smoothing unit, and power management unit for operating it at maximum extracted power called Maximum Power Point Tracker (MPPT). (Mastromauro et al, 2012) in their study described voltage and current control models using MPPT approach. Usually, PV systems are designed to operate at the point of maximum power called MPP in order to realize maximum efficiency and better utilization. Therefore, the need for MPPT module is an essential stage in energy conversion procedure to obtain maximum energy with reduced switching losses of the chopper and minimized overall system losses at high efficiency.

There are several MPPT techniques for tracking the maximum power of the PV system such as Perturb and Observation (P&O), which uses iteration procedures for reaching maximum power at the knee of power performance. (Femia et al, 2005) proposed optimization procedure for obtaining precise MPPT results. It is characterized by a simple mathematical approach and easy implantation, but with great voltage oscillation on the chopper electronic switch that cannot be completely avoided, leading to switching losses and excess of heat. The second technique is called Incremental Conductance (IC) method discussed by (Zegaoui, et al, 2011), which has a similar iteration procedure that uses the change of current rather than the change in power with respect to the voltage. The third technique is known as the Fuzzy Logic Control method (FLC) which was described by (Hasan et al, 2021) and is used very successfully in the implementation for MPP searching and the sliding mode control which was described by (Yatimi et al, 2016).

The P&O method stands out as the most relatively used method due to its simplicity. This method has a good operating behavior in slow changing solar irradiation and temperature change with respect to time. However, it is a time-consuming

*Corresponding Author's Email: *sameer@ppu.edu* (S. Khader)
URL: https://www.jree.ir/article_170661.html

Please cite this article as: Khader, S. & Daud, A. K. (2023). A Novel Approach to Fast Determining the Maximum Power Point Based on Photovoltaic Panel's Datasheet, *Journal of Renewable Energy and Environment (JREE)*, 10(4), 44-58. https://doi.org/10.30501/jree.2023.361697.1450.

2423-7469/© 2023 The Author(s). Published by MERC. This is an open access article under the CC BY license (https://creativecommons.org/licenses/by/4.0/legalcode).

method and hence, cannot track the MPP fast enough, leading to the loss of a certain amount of power before reaching the MPP value due to the iteration procedure and oscillation as well as generation of voltage stress across the chopper switch due to duty cycle variation.

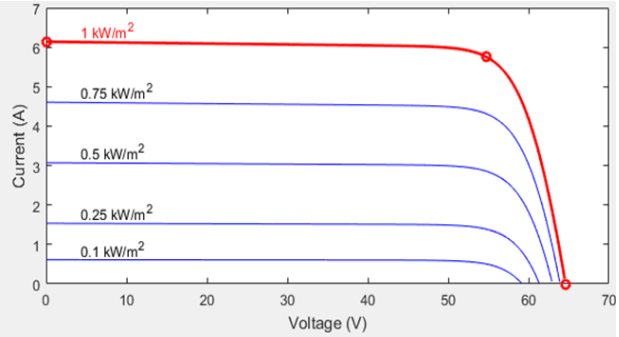

a) Panel P-V performance

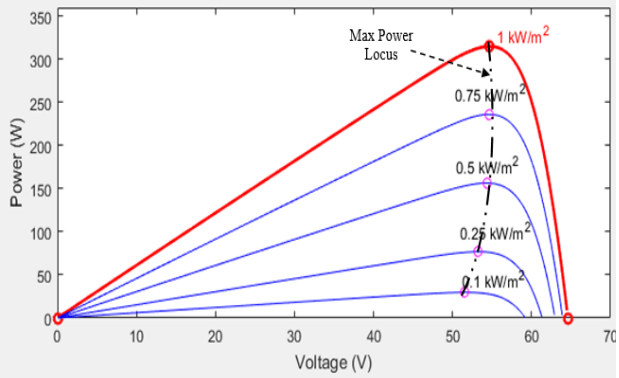

b) Panel I-V performance

Figure 1. Panel I-V and P-V characteristics.

Article main task and elements:

What is the article main task?

Usually, solar irradiation varies during the day time and this leads to continuous tracking of MPP point by various MPPT algorithms, meaning significant time delay, loss of energy, and excess of switching losses due to variation in the chopper duty cycle. Therefore, in order to avoid these drawbacks, it is necessary to immediately find the MPP voltage and power based on previously embedded equations V_{mpp} & P_{mpp} =f(G_T) for any irradiation rate during the day.

This article is organized as follows:

- Section 1: Introduction and overview about the development of electronic converters and their applications in solar energy and energy conversion.
- Section 2: Mathematical modeling for deriving a direct relationship between maximum power and solar irradiation using real data and specifications of manufactured solar panels.
- Section 3: Building the simulation model for direct detecting of the maximum power at any value of solar irradiation during the day time without oscillation around the MPP for Modified Single Primary Inductance Coil (MSEPIC) described by (Mahdavi et al, 2011) , (Bodetto et al, 2016) and (Fernão et al, 2016) .
- Section 4: Running the proposed model for simulation of power, voltage, and current at any time of the year without using the already known MPPT techniques.
- Section 5: Conducting various simulations for MPP power when the cell temperature varies below and above the Standard Test Conditions (STC) value.
- Section 6: Analysis of results and discussion are presented. Finally, some conclusions are drawn.

2. MATHEMATICAL MODELING

2.1. Panel's PV Current and Voltage

Most solar panel manufacturers provide the power voltage performance of a given real panel Ppv=f(Vpv) for solar irradiation starting with 100 Watt/m2 to 1000 Watt/m2 as shown in Figure 1, where the maximum values for voltage and power at the knee of the curves are stated in Table1 for SunPower-SPR-315E-WTH-D, (SUNPOWER datasheet, 2022).

With regard to the above issue for any type of PV panel, several methods can be used for MPP tracking. The only condition to build the required equation is to have PV data for small (may be minimum) and large (may be maximum) power spectra for a given type of panels. Table 2 presents the power range for various PV panel datasheets stored in MATLAB/Simulink database (MATLAB and Simulink (2016)).

Table 1. PV data at MPP for SPR315E-WHT-D.

G, Watt/m2	1000	750	500	250	100
Vmpp, V	54.7	54.65	54.34	53.38	51.64
Impp, A	5.76	4.32	2.88	1.44	0.576
Pmpp, Watt	315.1	236.1	156.5	76.88	29.75

In order to build the mathematical model and related simulation platforms, the following procedure is applied and graphically illustrated in Figure 2:

1. Read discrete values for the voltage and power of real solar panel and build the voltage performance Vmpp=f(G) and Pmpp=f(G) for irradiation points G=100, 250, 500, 750, and 1000 W/m^2.

Table 2. Examples of PV data at MPP for various panels at full Sun.

Panel Type	Range	Serial code	Vmpp, V	Impp, A	Pmpp, W
Sun Power	Small	SPR PL-PLT-63L-BLK-U	11.9	5.3	63.07
	Large	SPR-X20-445-Com	76.7	5.8	444.86
Canadian Solar	Small	CS5C-80M	17.5	4.58	80
	Large	CS7N-665MS	38.5	17.28	665
Soltech	Small	Soltech-1STH-215-P	29.35	7.34	215.1
	Large	Soltech-1STH-350-WH	43	8.15	350
Hanawa Q-cell	Small	Q-Cell 385	36.36	10.59	385
	Large	Q-Cell 585	45.10	12.97	585

2. Extract interpolation equations using MATLAB fitting tools for both voltage and power.
3. Build the continuous voltage equation V_{CON}=f(G) and P_{CON}=f(G).
4. Build/plot the continuous waveforms based on formulated equation for various panel datasheets.
5. Directly detect MPP for any given irradiation value.

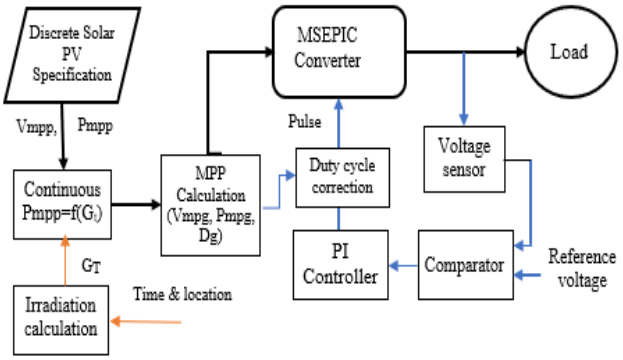

Figure 2. Model functional chart (Daud et al, 2022) .

where, $b_1 = 78.11;\ b_0 = 111.3$.

The obtained results related to voltage and power at MPP are displayed in Figure 4 for a power range of real panel types 1SOLTECH.

The same procedure is applied for another type of panels with a large power range related to HANAWA Q-Cell (Hanawa-Q Cell, 2022) , where the maximum rated panel power is 585 Watts peak with a rated voltage of 45V per panel, as shown in Figure 5, for which the voltage and power variation is displayed at MPP, as the solar irradiation varies as well.

2.3. Direct Detection of MPP`

After deriving the continuous voltage and power equations with respect to the solar irradiation, there is a need to derive a formula for directly determining the chopper duty cycle, voltage, and power at MPP without conducting any type of iteration procedures. To this end, it is necessary to determine the minimum power at a minimum irradiation rate, e.g., G=100W/m^2, and the rated panel power at G=1000W/m^2 is already known from the datasheet. With reference to Figure 4 (b), the MPP powers of performance 1 and performance 5 are known and represented in Figure 6, which are used to derive the power formula for two options:

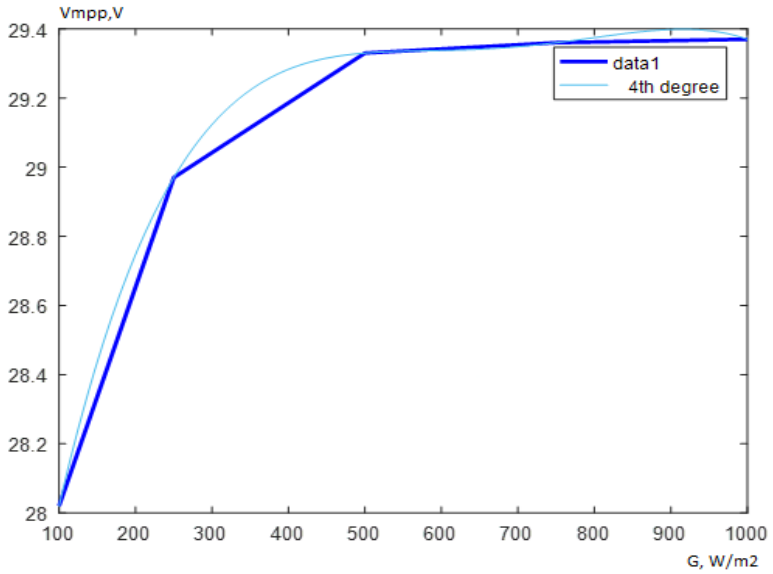

Figure 3. Vmpp at different irradiation rates.

6. Build the solar irradiation rate G=f(time) for any time of the year.
7. Combine the obtained equation V_{CON} and P_{CON} with G.
8. Build the Simulink model that combines the MPP performance with irradiation for any time of the year,

determine MPP for Pmpp and Vmpp at any value of G, and plot Vmpp and Pmpp=f(G).

2.2. Voltage and Power Equations`

Let us start with the data specification related to Solar panel Soltech-15TH-215-P, where the voltage is displayed in Figure 3 with the interpolated equation stated in (1), while the power performance versus irradiation has a linear change presented as a first-order equation. It is shown that the MPP voltage has a slight change when the irradiation varies between a weak and a full sun. The interpolated voltage equation is presented as follows:

$$V_{MPP} = \alpha_4 Z_V^4 + \alpha_3 Z_V^3 + \alpha_2 Z_V^2 + \alpha_1 Z_V + \alpha_0; \quad (1)$$

where, $Z_V = \left(\frac{G_T - \beta}{\delta}\right);\ \beta = 520;\ \delta = 370;$

$\alpha_4 = -0.23;\ \alpha_3 = 0.42;\ \alpha_2 = -0.17;\ \alpha_1 = 0.041;\ \alpha_0 = 29.$

While the power equation can be stated as follows:

$$P_{MPP} = b_1 Z_V + b_0; \quad (2)$$

Option 1: When the rated panel power $\mathbf{P_{mpp,\,i}}$ is located inside the power range "Performance A", the minimum power $\mathbf{P_{min,i}}$ is determined according to the following equation:

$$P_{min,i} = (P_{max,i} - P_{maxs})X_p + P_{mins} \quad (3)$$

where, $X_p = \frac{P_{minL} - P_{mins}}{P_{maxL} - P_{maxs}}$ presents the power ration of panel spectrum,

P_{mins}, P_{maxs}: the smallest min. and max. values of rated Pmpp of PV Panel's power range;

P_{mimL}, P_{maxL}: the largest min. and max. values of rated Pmpp of PV Panel's power range;

P_{mini}, $P_{max,i}$: the min. and max. values of rated Pmpp inside of PV Panel's power range;

$P_{min,o}$; $P_{max,o}$: the min. and max. values of rated Pmpp outside of PV Panel's power range.

Option 2: When the panel power $\mathbf{P_{mpp,o}}$ is located outside the power range "Performance **B**", the minimum power $\mathbf{P_{min,o}}$ is determined according to the following equation:

$$P_{min,o} = P_{max,o}X_p + \frac{\Delta P}{P_{maxL} - P_{maxs}}, \quad (4)$$

with, $\Delta P = P_{maxL} \cdot P_{mins} - P_{maxs} \cdot P_{minL}$

The instantaneous maximum power P_{mpp} (G) at given irradiation can be expressed as follows:

$$P_{mpp}(G) = M.(G - G_{min}) + P_{min} \quad (5)$$

with, $M = \frac{P_{max} - P_{min}}{G_{max} - G_{min}}$; presents the power slope.

and

$$P_{max} = \begin{cases} P_{max,i} & \text{for case 1} \\ P_{max,o} & \text{for case 2} \end{cases} \text{ and } P_{min} = \begin{cases} P_{min,i} & \text{for case 1} \\ P_{min,o} & \text{for case 2} \end{cases}$$

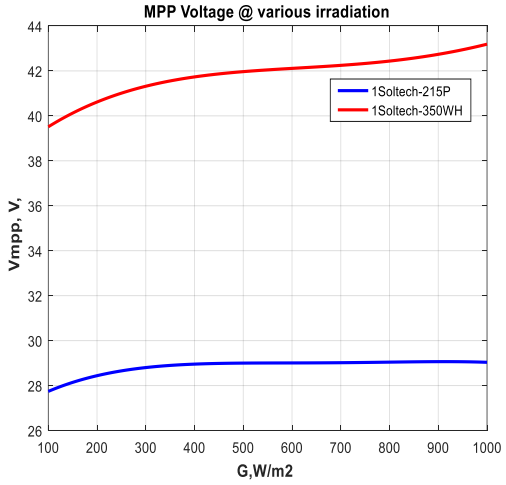

a) Voltage at MPP

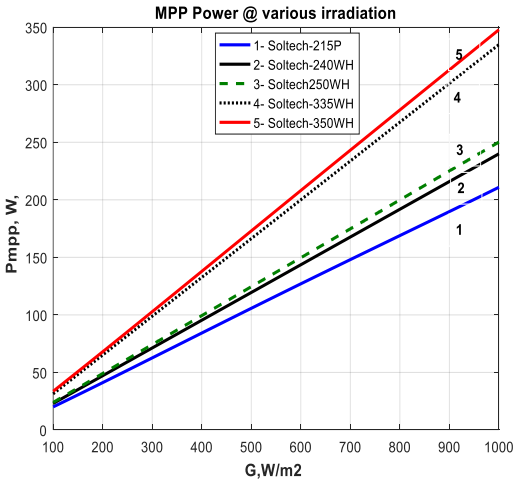

b) Power at MPP

Figure 4. Voltage and power at MPP for different irradiations of various SOLTECH panels.

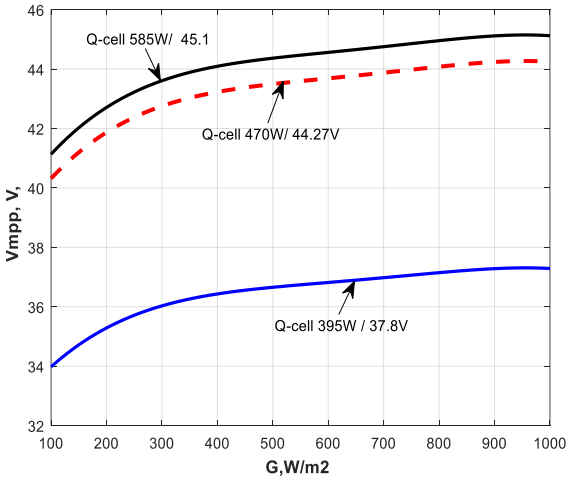

a) Voltage at MPP

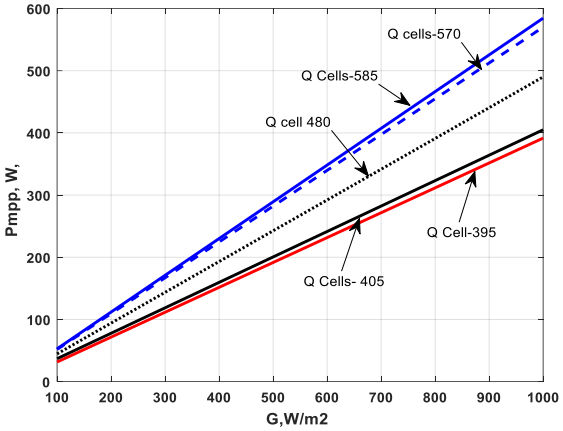

b) Power at MPP

Figure 5. Voltage and power at MPP for different irradiations of HANAWA Q-Cell (Hanawa-Q Cell, 2022).

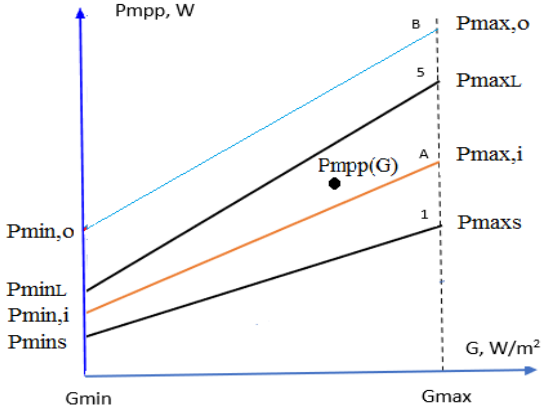

Figure 6. Exact MPP power at given G.

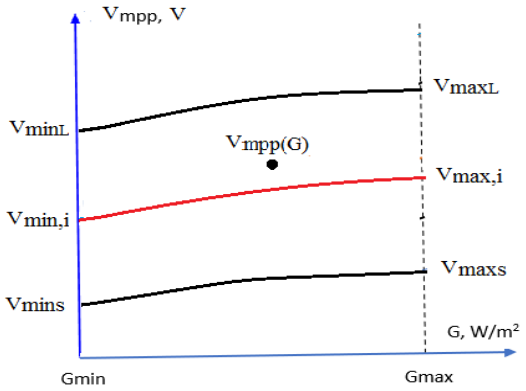

Figure 7. Exact MPP voltage at given G.

Referring to Figure 7, the MPP voltage V_{mpp} of PV panel within the power range can be calculated via the following voltage formula:

$$V_{mpp}(G)=\left(a_{4s}\cdot Z_V^4+a_{3s}\cdot Z_V^3+a_{2s}\cdot Z_V^2+a_{1s}\cdot Z_V+a_{0s}\right) \quad (6)$$

With

$$X_{V,i}=X_y\cdot\left[1+\alpha_p\cdot X_z\cdot\left(\frac{V_{minL}-V_{mins}}{V_{minL}+V_{mins}}\right)\right]$$

$$X_y=\frac{V_{max,i}}{V_{maxs}} \quad \text{and} \quad X_z=\frac{V_{maxL}}{V_{maxs}}.$$

$$\alpha_p=\text{f (Panel type)}\ \le 1\ .$$

Where, V_{mins}, V_{maxs}: the min. and max. values of rated Vmpp of PV Panel's power range;
V_{mimL}, V_{maxL}: the largest min. and max. values of rated Vmpp of PV Panel's power range;
$V_{min,i}$, $V_{max,i}$: the min. and max. values of rated Vmpp inside of PV Panel's power range;
a_{os}, a_{1s}, a_{2s}, a_{3s}, a_{4s}: Equation coefficient of the smallest power of PV panel power range;
α_P: Panel type's tuning coefficient (estimated value).
Equation (6) is applied for different panel types in order to determine the Vmpp voltage at any irradiation rate and panel's specification. Figure 8 shows the behaviors of Vmpp(G) for some well-known solar panels worldwide as stated (Robert Wortrich, 2022), keeping in mind that the rated power is selected to be 350W for all types.

It is clearly shown that Vmpp for the same radiation differs from one type to another with a percentage of change that goes up to 17%, as shown in the stated histogram.

It is imperative to look at the power behavior as shown in Figure 9 where all panel types have the same rated power of 350W. Now, by studying these performances, it can be noticed that there is a slight difference in the generated voltage and power amongst several types.
Based on the voltage generation according to Figure 8, the panel type "SunPower" had the highest value, while "Canadian" had the lowest value.

Based on the generated power according to Figure 9(b), it can be noticed that the panel type "Trina" generated the largest amount of energy. Therefore, the application of this approach provides clear information about the effectiveness of panels and helps better judge in the selection process.

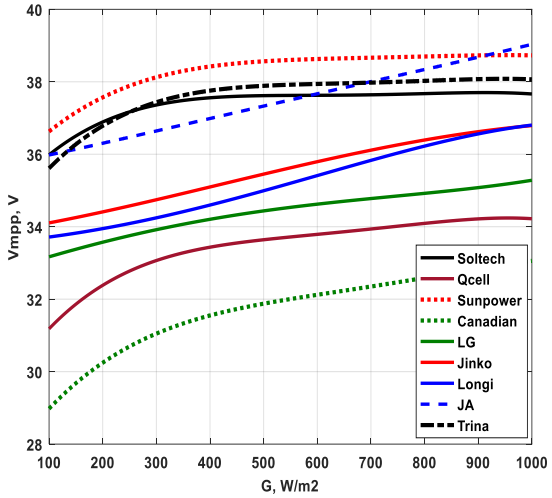

a) Continuous change of Vmpp

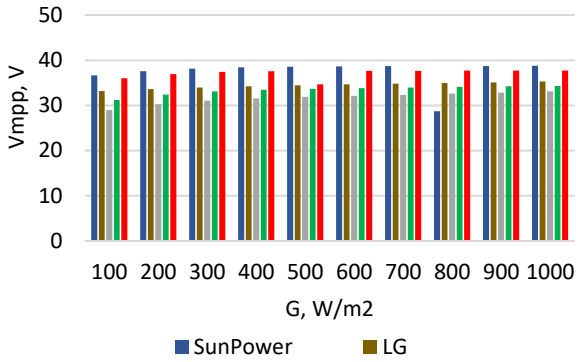

b) Histogram of selected 5 panels.

Figure 8. V_{MPP} voltage performance for various panel types with Pmpp=350W

2.4. Solar Irradiation Calculation

In order to determine the maximum power at given irradiation, it is necessary to determine the daily solar irradiation any time of the year as stated in (Gilbert M. Masters, 2017) as follows:

- The direct solar irradiation is given by:

$$G(t)=G_{max}\sin\left(\frac{\pi}{T_d}(t-t_{sr})\right);\text{for } t_{sr}\le t\le t_{sr}+T_d \quad (7)$$

where, t_{sr}, t_{ss}, T_d are the sunrise time, sunset time, and day duration, respectively.

$$t_{sr}=LT-\frac{T_d}{2}\ ;LT=LST-\frac{TC}{60}\ ;\ t_{ss}=LT+\frac{T_d}{2}\ ; \quad (8)$$

In addition, the daily duration can be presents as :

$$T_d=\frac{2}{15}\cos^{-1}(-\tan\phi\tan\delta)\ ; \quad (9)$$

where

$$\delta=23.45*\sin\left[\frac{360}{365}(n-81)\right].$$

ϕ=31.53° is the solar latitude;
n- is the day number ($1\le n\le 365$); and
LST and LT are the local solar time and local time, respectively.

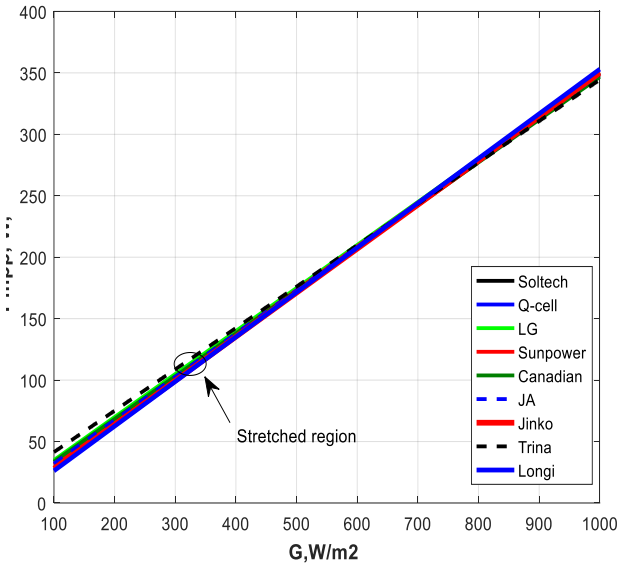

a) Full irradiation range

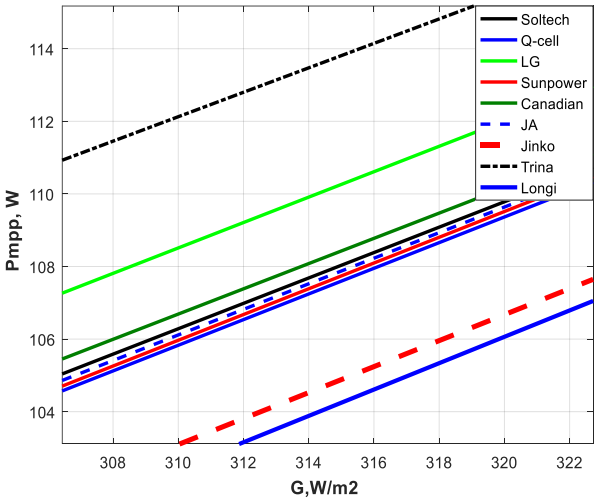

b) Stretched irradiation range.

Figure 9. P_{mpp} power performance for various panels' types.

The local time LT can be expressed as follows:

$$LT = 4 * (\varphi - LSTM) + EOT. \quad (10)$$

where φ= 35.1° is the longitude angle;
LSTM=15°.ΔTUC is the local standard time meridian;

$$EOT = 9.87 * \sin 2\beta - 7.53 * \cos\beta - 1.53 * \sin\beta; \quad (11)$$

where

$$\beta = \frac{360}{364}(n - 81).$$

3. SIMULATION RESULTS AND DISCUSSIONS

The derived equations for solar irradiation, power, and duty cycle at MPP are simulated using MATLAB/ SIMULINK platform for MSEPIC shown in Figure 10(a) where the conventional SEPIC converter circuit is also displayed. The built simulation model is illustrated in Figure 10(b), while Figures 10(c) to 10(j) illustrate the sub-models used in conducting the simulation process. The obtained results are hereby displayed:

3.1 Continuous Values Approach

The calculation of the MPP voltage and power based on discrete irradiation values yields a step-wide change in the voltage and power, which is somewhat far from real conditions, as shown in Figure 11 (and according to Table 1). In contrast, applying a continuous-value approach to calculating the voltage and power throughout the complete solar irradiation range yields closer results to those of real irradiation conditions.

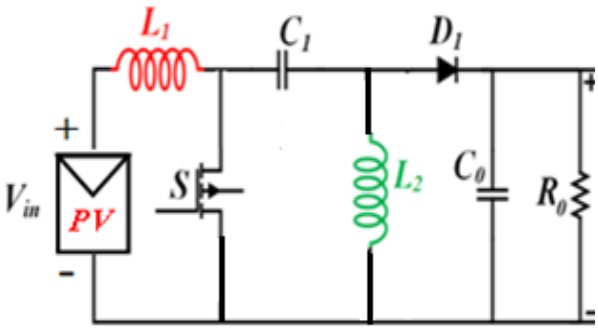

a1) SEPIC Converter

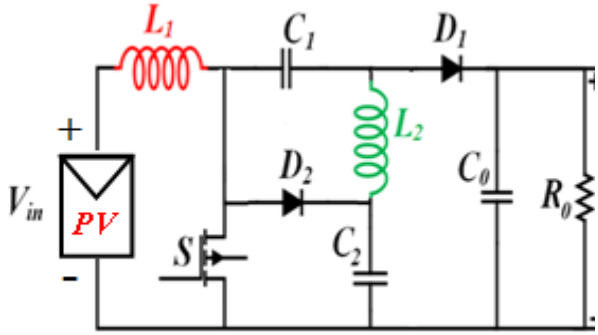

a2) Modified SEPIC Converter

(a) SEPIC and Modified SEPIC (Daud et al, 2022)

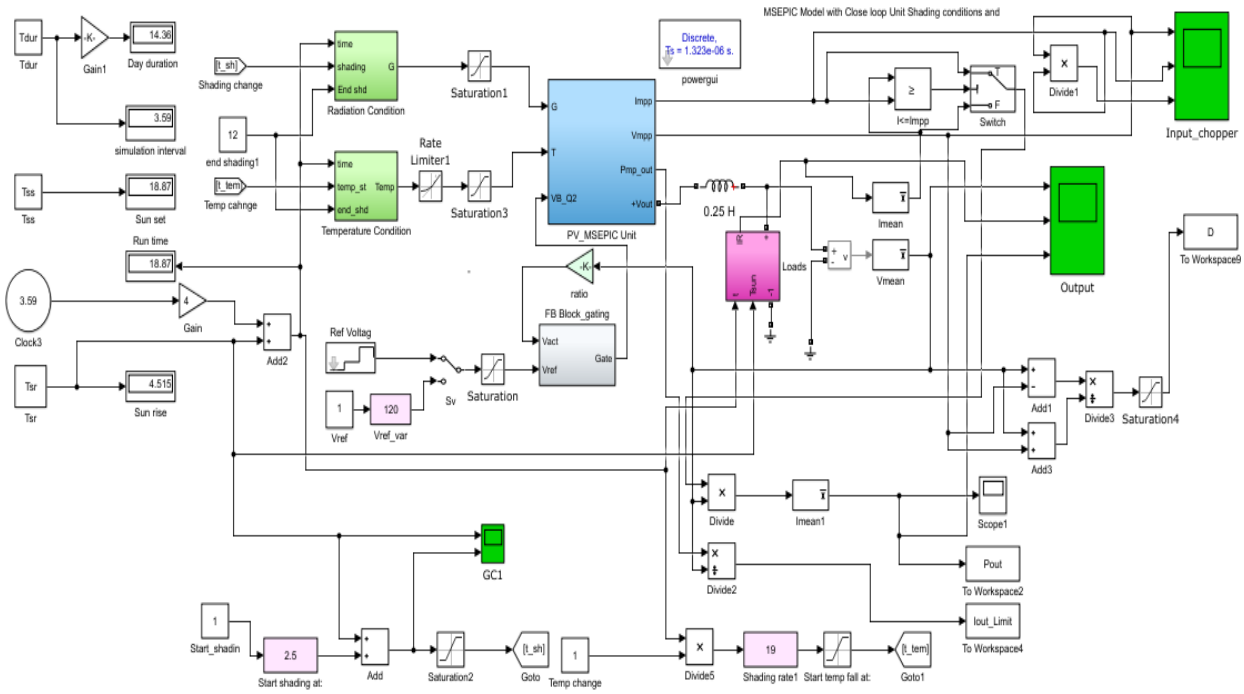

(b) Main Matlab/ Simulink Model

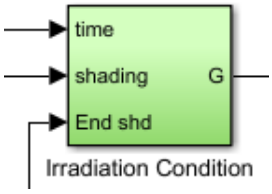

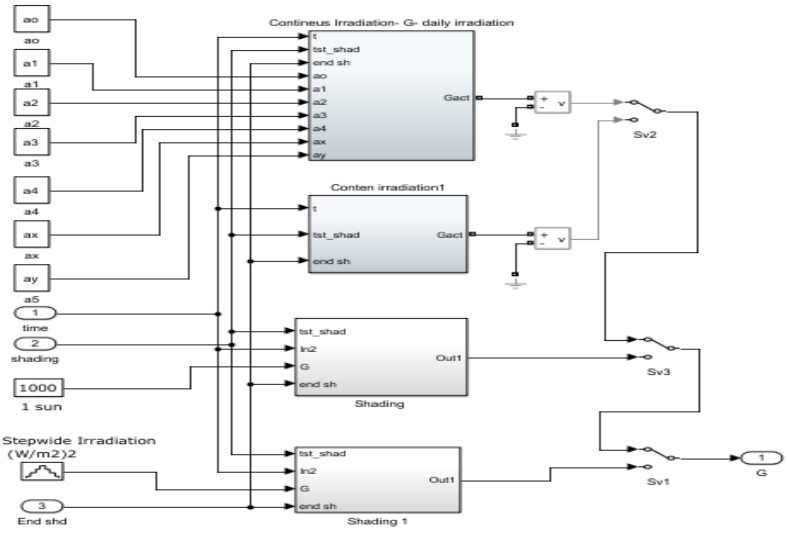

(c) IrradiationCoditions sub-model with a shading unit

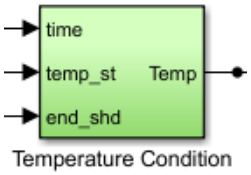

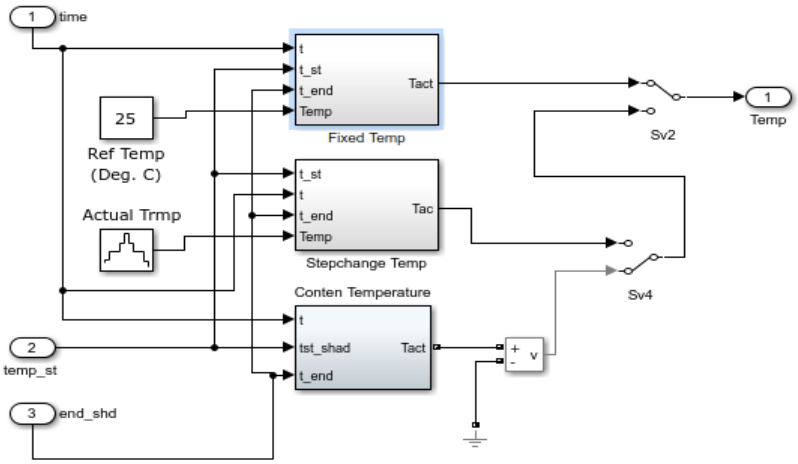

(d) Temperature Condtion sub-model

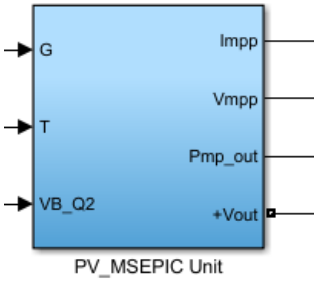

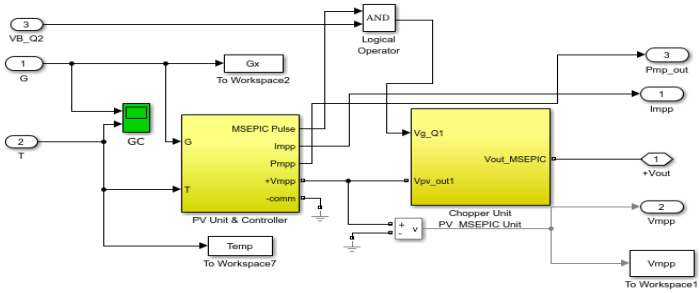

(e) PV & MSEPIC Chopper sub-models

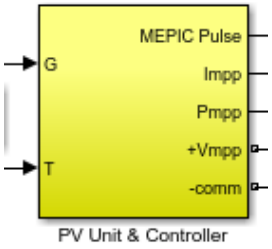

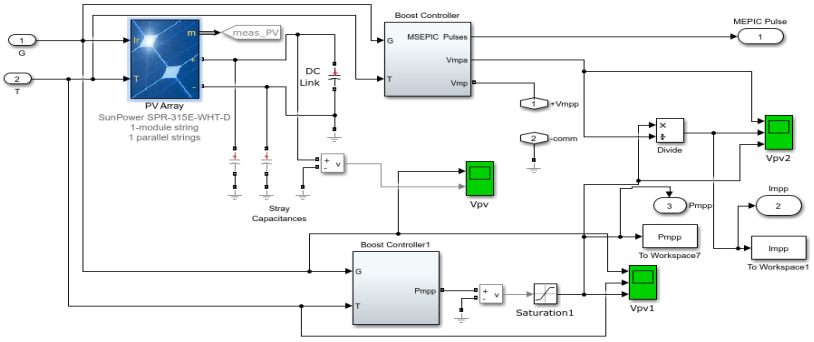

(f) PV Panel and MSEPIC controller

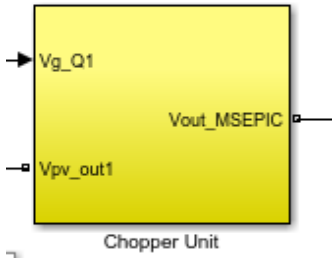

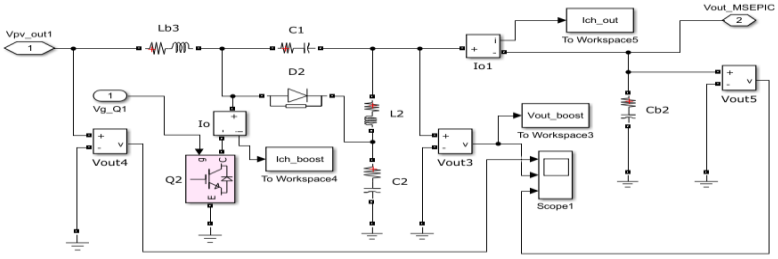

(g) MSEPIC simulation circuit

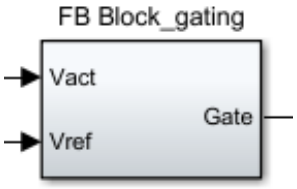

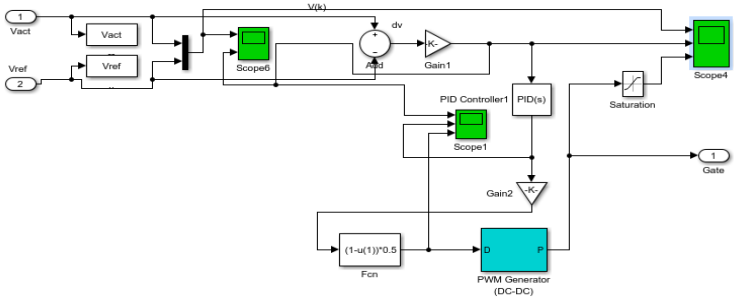

(h) Close-loop control with PID controlle

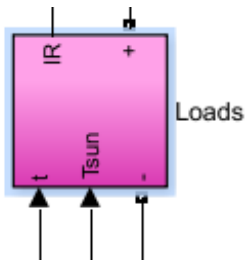

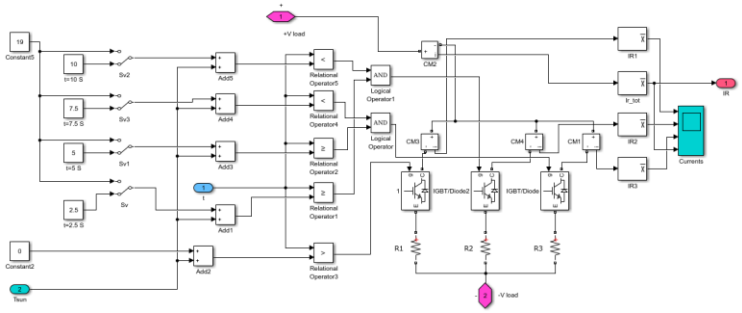

(i) Loading unit with R1, R2, and R3.

Figure 10. Electrical and simulation main and sub-modules.

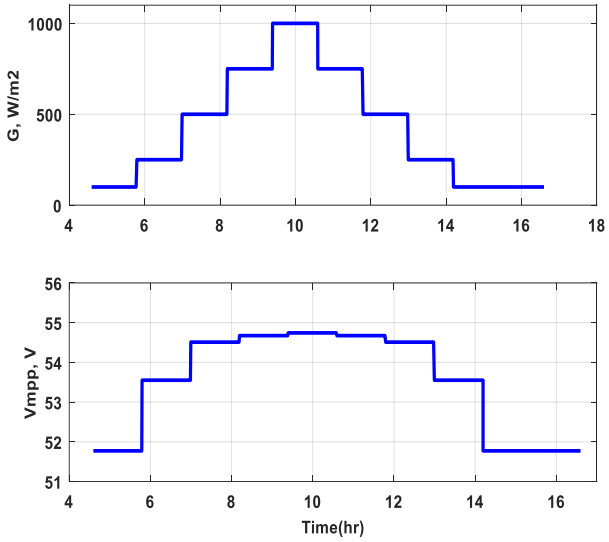

Figure11. Discrete values of solar irradiation and voltage at MPP.

Figure 12 illustrates the MPP voltage and power change, Vmpp, Pmpp=f(GT) with respect to the daily irradiation for both the 21st dates of June & December. It is shown that the day duration changes from June to December and related MPP voltage and power vary as well in standard test conditions.

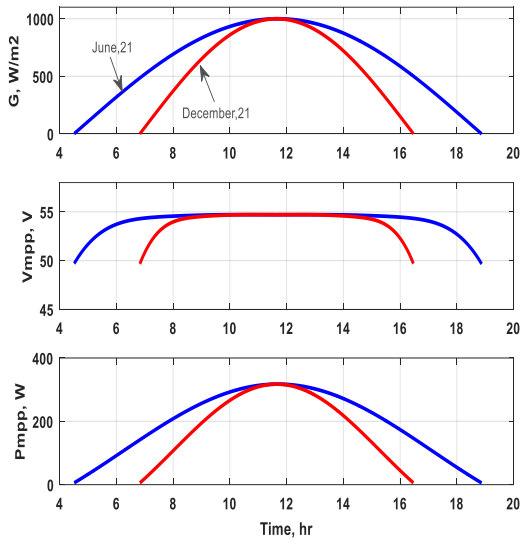

Figure 12. MPP voltage & power for the longest & shotest days of the year.

Figure13 illustrates the loading scenario in which the current changes according to connected loads and this current is projected over the panel capability with respect to MPP current for the same months. It is shown that a significant current shortage is observed during December month when Impp<Lout.

Figure 14 illustrates the effect of load changing over the output voltage at various irradiation rates for 21st June, in which it can be noticed that the negligible oscillation of the output voltage during the transition from one loading level to another.

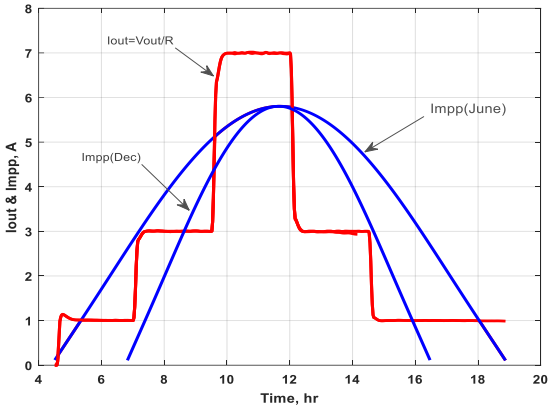

Figure13. Matching between load current (load changing) and MPP current.

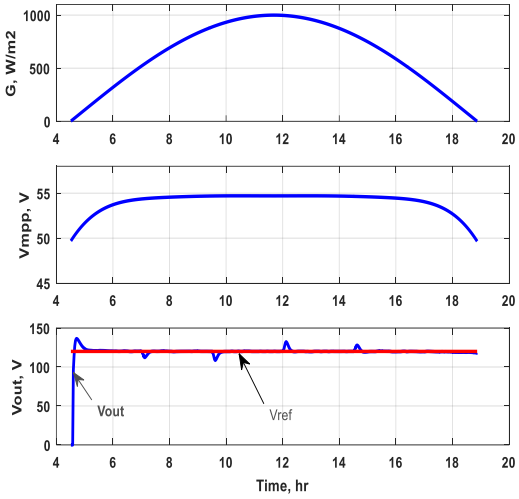

Figure 14. Output and reference voltage change.

3.2 MPP Power and Current for Real Measured Irradiation Data.

The proposed MPP approach is now applied for real measured data taken from a weather station installed over the rootop of the university buildings where the irradiation rate for May, 23,2022 is shown in Figure 15, but the real temperature measured for the same date is shown in Figure 16 (Solar Log 2000, 2022). The generated equations for irradiation (G) and temperature (Tt) are stated in (12) and (13) as follows.

$$G = \delta_4 Z_g^4 + \delta_3 Z_g^3 + \delta_2 Z_g^2 + \delta_1 Z_g + \delta_0; \quad (12)$$

where,

$$Z_g = \left(\frac{t - \beta_1}{\beta_{12}}\right);\ \beta_1 = 11.61;\quad \beta_2 = 4.062;$$
$$\delta_0 = 999.6;\ \delta_1 = 1.441e-13;\ \delta_2 = -410.71;$$
$$\delta_3 = 2.491e-14;\ \delta_4 = 25.46\ .$$

and

$$T_t = \tau_4 Z_t^4 + \tau_3 Z_t^3 + \tau_2 Z_t^2 + \delta_1 Z_t + \tau_0;$$

where,

$$Z_t = \left(\frac{t - \beta_\tau}{\delta_\tau}\right);\ \beta_\tau = 1.60;\quad \delta_\tau = 0.88;$$
$$\tau_0 = 19;\ 3.2;\ \tau_1 = 3.2;\ \tau_2 = -2.4;$$
$$\tau_3 = 3.2;\ \tau_4 = 0.21\ . \quad (13)$$

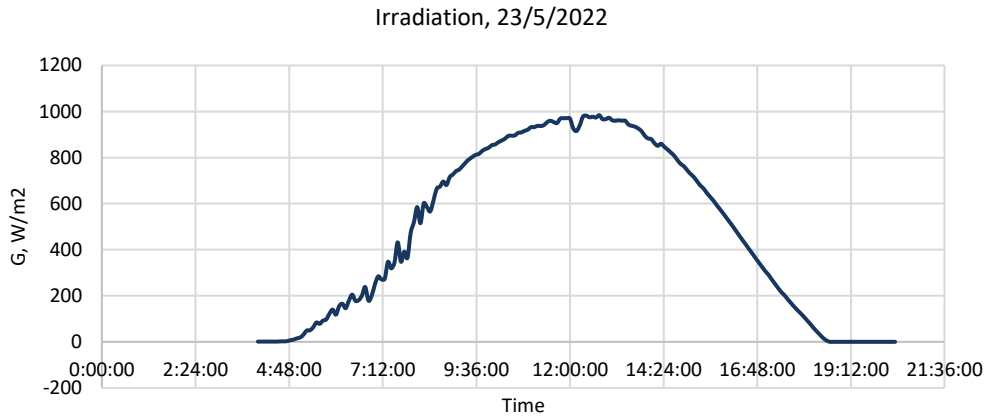

Figure 15. Measured real irradiation .

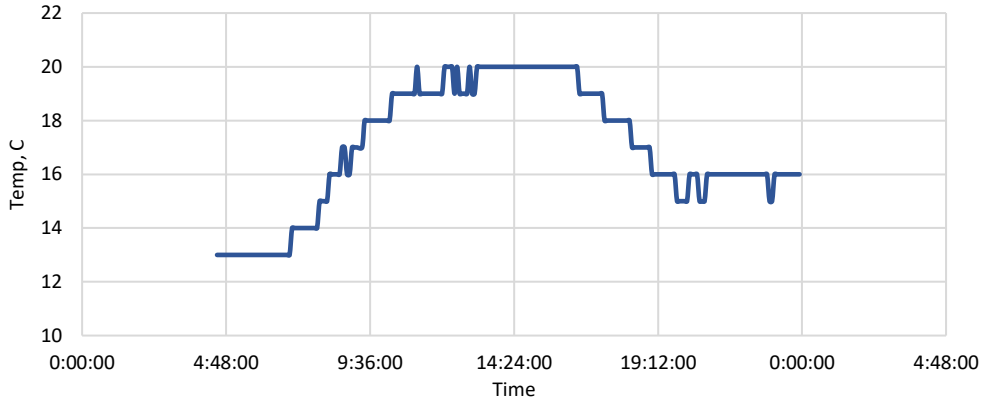

Figure 16. Measured real temperature..

After generating approximated equations for both irradiation and temperature, the MPP volage and power (Daud et al, 2022) are expressed according to (14) and (15) and displayed in Figure 17, taking into account the effect of temperature change for performance test conditions.

$$V_{MPP}(T_t) = V_{MPP}(STC) * \left[1 - \frac{\Delta V}{^\circ C}(T_t - 25)\right]; \quad (14)$$

$$P_{MPP}(T_t) = P_{MPP}(STC) * \left[1 - \frac{\Delta P}{^\circ C}(T_t - 25)\right]. \quad (15)$$

where

$$\frac{\Delta V}{^\circ C} = -0.27269\% \frac{V}{^\circ C}; \quad \frac{\Delta P}{^\circ C} = -0.016823\,\% \frac{W}{^\circ C_4}$$

V_{MPP} (STC) and P_{MPP} (STC) are the rated panel voltage and power in full sun and standard test conditions.

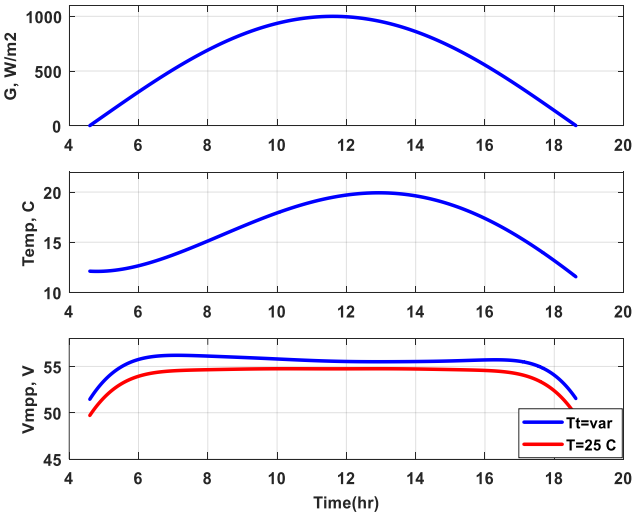

Figure 17. MPP voltage at different irradiations and temperature Tt.

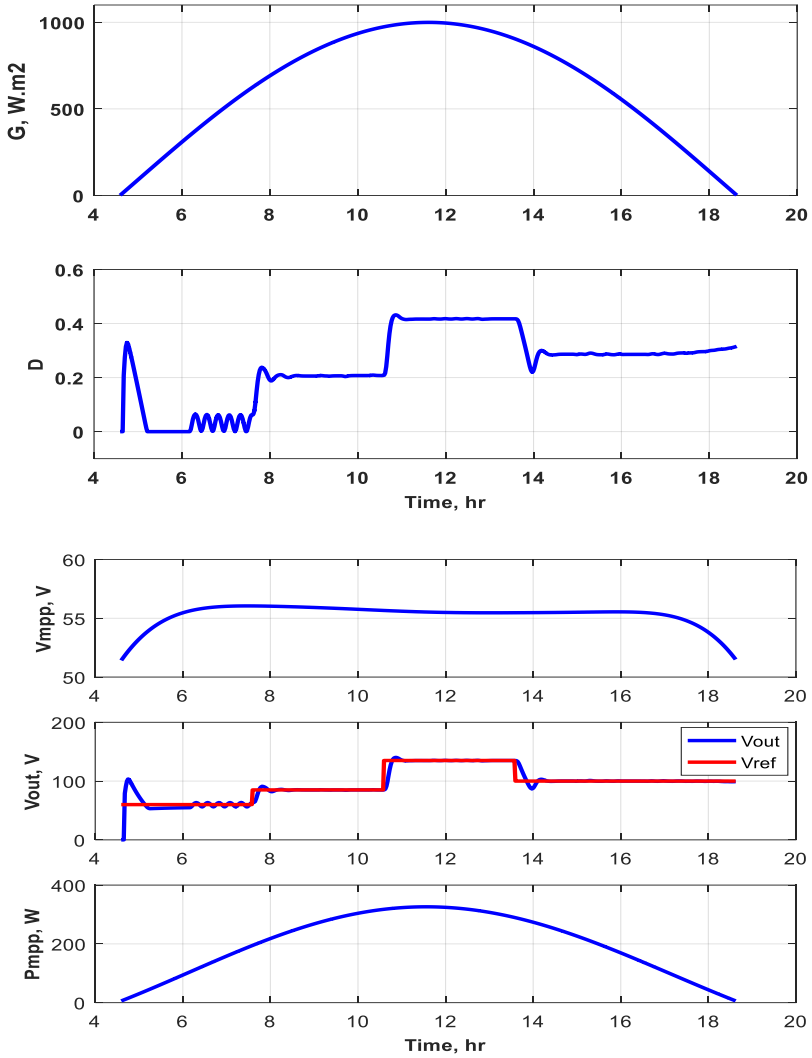

a) Main performances in the time domain

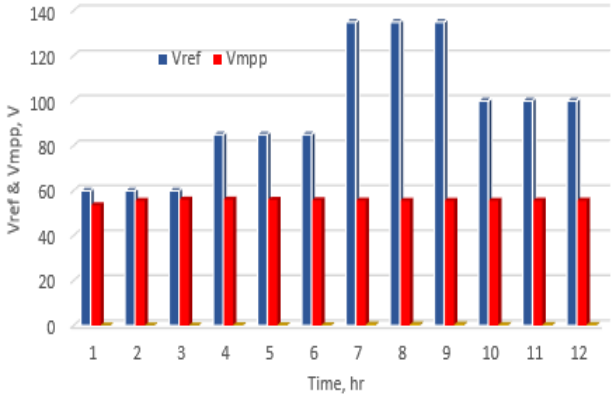

b) Histogram of voltages

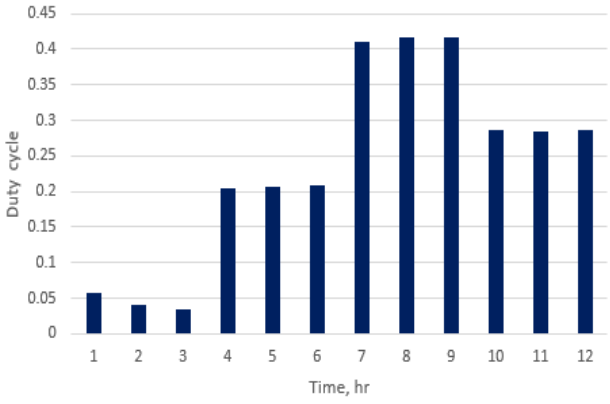

c) Histogram od duty cycle

Figure 18. Input-output performances at different loading voltages for May,23rd, 2022.

It can be noticed that the MPP voltage is higher than that of STC because the maximum temperature for that day (May 23rd , 2022) was detected around 20°C at noon time.

Figure 18 illustrates both the input-output performances in terms of irradiation, duty cycle, MPP voltage, and output voltage according to reference voltage with values V_{REF}= 60, 85, 135, and 100 V and with constant load of R=120 Ω.

In addition, the histogram for the voltage and duty cycle is displayed in the same figure.

The MSEPIC chopper duty cycle is expressed according to (16) in order to generate PWM pulses capable to regulate and boost up the MPP voltage according to the reference values mentioned by (Daud et al, 2022) :

$$D(t) = \frac{V_{REF}-V_{MPP}}{V_{REF}+V_{MPP}}. \quad (16)$$

It can be seen that at a low output reference voltage, the average duty cycle is tolerating around zero, i.e., D≅0, while at a high output reference voltage, where the difference between (V_{REF}-V_{MPP}) is high which requires the chopper to operate at a larger duty cycle, i.e., D≅0.42.

4. MPP TECHNIQUES COMPARISON WITH THE PRESENT APPROACH

There are several MPPT techniques used to operate the chopper at maximum power of the PV system as proposed in (Ben Ali et al,2022), (Pavithra et al, 2021) ,(Hossain et al, 2021), (Chowdhury et al, 2021) and (Boonraksa et al, 2022), where four techniques are described in this work as follows: Hill Climbing (HC), Incremental Conductance (INC), Perturb and Observe (P&O), and Fuzzy Logic Control (FLC).

These techniques have their pros and cons with respect to the fast response, starting time, output power variation, occurred chopper losses, and model simplicity. Three key decision elements can be taken for criteria judgment and precise estimation proposed by already conducted research done by Eltamaly and Rizk (Eltamaly et al, 2015) over solar panel type "Solarex MSX-60 "with data stated in Table 3.

Table 3 The key specifications for the Solarex MSX60 PV panel (Solarex PV Specifications, 2022) .

Vmpp,V	17.1	Voc, V	21
Impp, A	3.5	Isc, A	3.74
Pmpp, Watt	59.90	T, C	25

4.1. Starting Time

This is the time taken from the instant where the radiation changes till reaching the MPP value. Any significant increase in this time should cause additional energy loss and voltage stress over the chopper switch and excess of heat.

The variation of the generated PV power and duty cycle during starting time for mentioned techniques are illustrated in Figure 19, where all of them reach the maximum power Pmax within the time $\mathbf{t_{start}}$=**0.2** second.

While according to the present approach, there is no significant time to reach the maximum power under clear sky conditions as shown in Figure 20, i.e., $\mathbf{t_{st}} \cong$ **0.05** second.

4.2. Output Power Variation

As the solar irradiation varies, the generated MPP changes, as shown in Figure 21, for the mentioned techniques stated in (Eltamaly et al, 2015), where the observed uneven oscillation in duty cycle and power perturbation around the maximum value of the power point cause additional chopper losses due to frequent switching on and off.

These behaviors can be minimized through our proposed

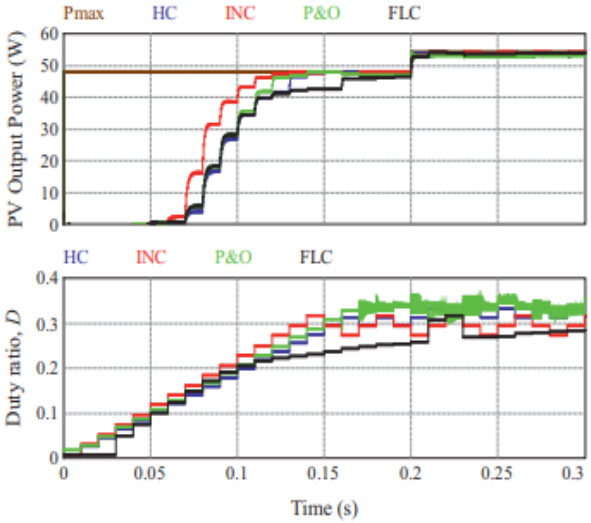

Figure 19. Power and duty cycle presented in (Eltamaly et al, 2015)

approach, as shown in Figure 22, for the constant reference

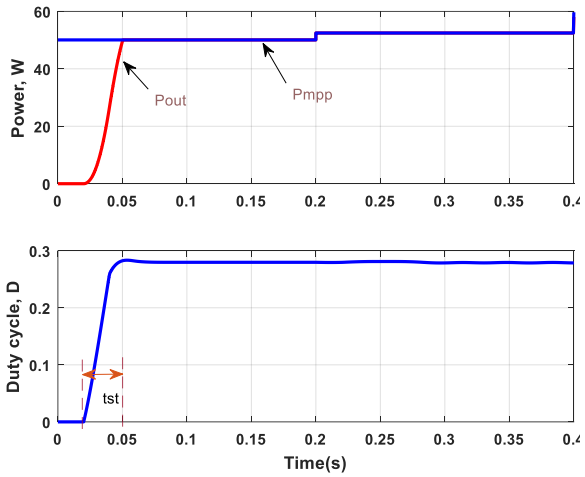

Figure 20. The power and parameters of the proposed approach in the full sun condition.

voltage of V_{ref}=30V and fixed load of R_1=15.5 Ω, where the irradiation changes 800, 850, and 1000 W/m^2.

It can be shown that the duty cycle varies within a small range with an average value of D_{avg}= 0.28.

Comparing the P&O algorithm of Figure 21 in terms of duty cycle with that of Figure 22, a stable change of D irrespective of the great change in solar irradiation during the day can be observed.

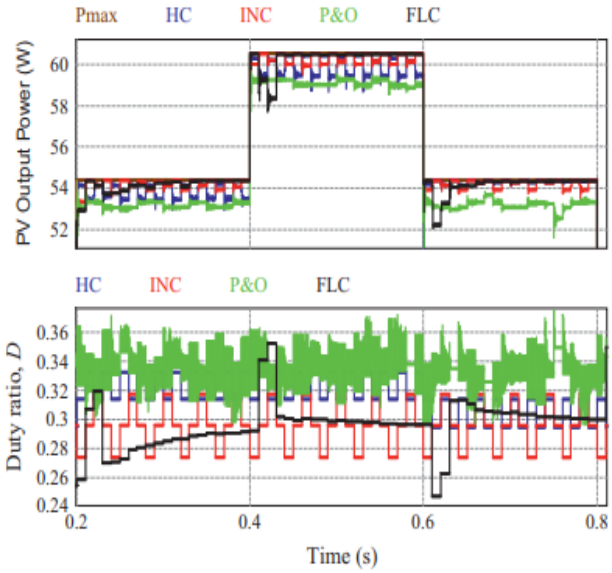

Figure 21. MPP power and duty cycle with variable irradiation described in (Eltamaly et al, 2015).

The above-mentioned techniques deal with a step-wide change in solar irradiations during the day being somewhat far from the real case of solar irradiation except in the case of sudden shadowing of the panel. Our proposed approach deals with a continuous change in solar irradiation, which causes further reduction in voltage stress across the chopper switch and conditioning elements of another chopper.

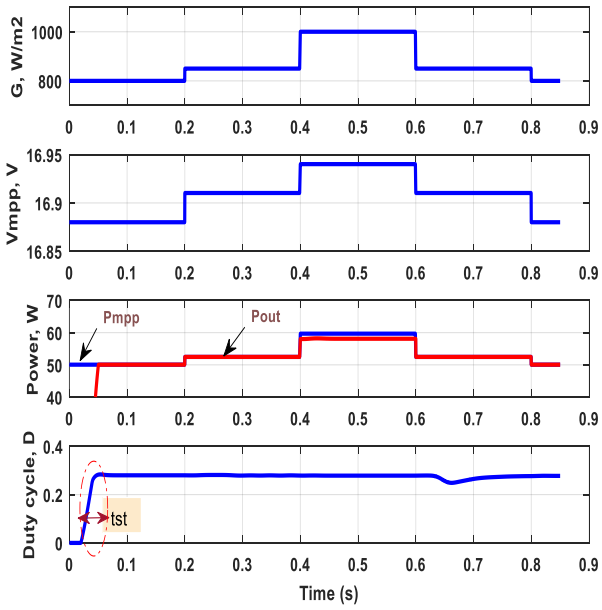

Figure 22. Main parameters of the proposed approach at different irradiation rates

5. CONTINUOUS CHARACTER OF MAXIMUM POWER AT A FIXED OUTPUT VOLTAGE

Figure 23(a) shows the continuous character of solar irradiation and corresponding reference voltage V_{out} = 20, 35, 50, and 40 V with a fixed load of R_1=60Ω , while Figure 23(b) shows the

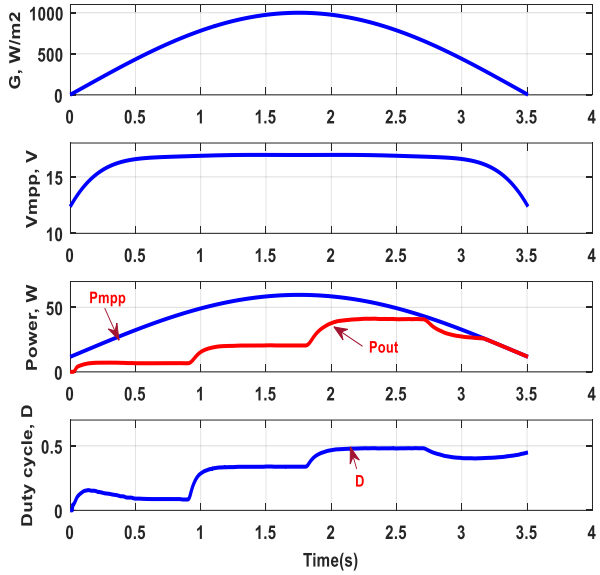

a) With variable output voltage and fixed load of R_1=60 Ω..

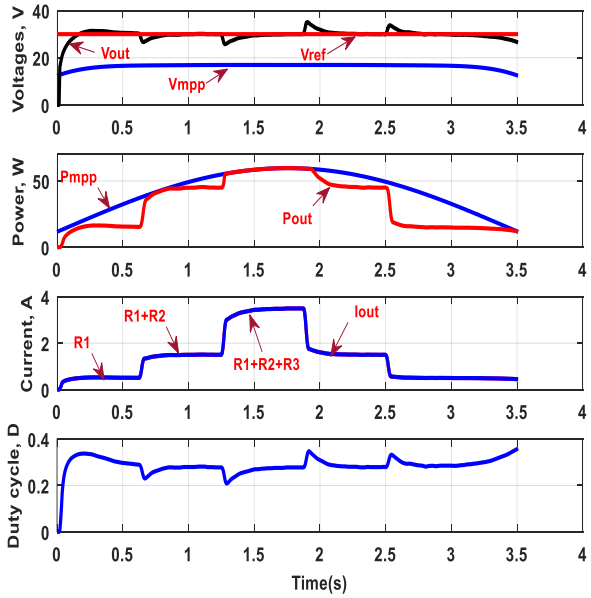

b) With fixed output voltage and variable loading of R_1, R_2, and R_3.

Figure 23. Main parameters of the proposed approach to continuous irradiation.

case when Vref=30V and the load varying with R_1=60Ω, R_2=30Ω, and R_3=15Ω.

It can be shown that keeping the voltage at a fixed reference value reduces the oscillations of the duty cycle and the load voltage. Furthermore, when various loads are added, the voltage sag is immediately recovered and the system returns to deliver an exact and stable output voltage.

6. CONCLUSION

A novel approach was applied to extract power at MPP without the need for conventional MPPT techniques. The proposed technique outperforms the conventional ones by eliminating the time needed to reach the point of maximum power and the

consequent loss of energy. In addition, frequent switching and voltage tension across the switching device were reduced.

The proposed approach used the PV key specification provided by the panel's manufacturer at different irradiation rates, where a continuous power function was derived for MPP points without running any kind of iteration procedures. The derived equation remained valid and regenerated itself for other panel data that belonged to the same manufacturer datasheet.

The PV power performance was built for any rated value of manufacturer's datasheet by merely noting the rated panel power. A variable loading was simulated at which the power, voltage, and current were tracked at the MPP.

The proposed model validation was verified based on the real measured data for solar irradiation and panel temperature. Furthermore, this model was compared to other published data in terms of the starting time and power fluctuations around the MPP (Eltamaly et al, 2015) .

Accordingly, the data published from used algorithms were reported around 0.2 second, while the starting time of our proposed model tended to about 0.05 second. Furthermore, the voltage stress and switching losses were significantly reduced.

The proposed model was projected over PV datasheets of nine solar companies with respect to the power and voltage at MPP, where a comparison analysis was conducted. The results showed a significant difference between these panels in terms of voltage and power at MPP, which in turn gave us a clear decision about panel selection.

The importance of the proposed model for the PV system manufacturers lies in reducing hardware complexity in the process of fabricating MPPT module and related accessories. Mainly, there is no need for voltage and current sensors to measure the PV voltage and current and no need for complicated microprocessor module, too. Furthermore, increase in the chopper lifetime due to reduced voltage stress was achieved besides reduced heatsink size. Given the reduction of the model complexity, the overall solar inverter performances were enhanced and the system footprint (size) and cost were achieved. The only restriction was that this model was valid for clear sky conditions with neglected effect of dust and eventual mismatching.

For future research, a hardware prototype model should be built and experimentally implemented in order to practically validate the discussed analytical and simulation results. This should be the main objective of the upcoming article.

CONFLICT OF INTEREST

The authors declare no conflicts of interest regarding the publication of this paper.

AUTHOR CONTRIBUTIONS

Sameer Khader implemented the SIMULINK model and presented building performances, conclusions, and paper preparation.

Abdel-Karim Daud carried out the mathematical model, analyzed the numerical results, discussed the results, and helped finalize the paper.

NOMENCLATURE

MPP	Maximum Power Point
MSEPIC	Modified Single Ended Coil
LSTM	Local Standard Time Meridian (hour)
ΔTUC	Differential Universal Coordinated Time
LT	Local Time (hour)
LST	Local Standard Time (hour)
EoT	Equation of Time (minute)
PV	Photovoltaic
STC	Standard test conditions
MPPT	Maximum Power Point Tracker
FLC	Fuzzy Logic Control
INC	Incremental Conductance
HC	Hill Climbing
P&O	Perturb and observe
Greek letters	
δ	declination angle (degree)
Φ	Latitude angle (degree)
φ	Longitude angle (degree)
β	Parameter depends on the day number (degree).

REFERENCES

1. Ben Ali, I., Naouar, M.W. & Monmasson, E. (June, 2022). Parameters identification for a photovoltaic module: comparison between PSO, GA and CS metaheuristic optimization algorithms. *INDERSCIENCE*, 211-230. https://doi.org/10.1504/IJMIC.2021.123378

2. Bodetto, M., et al. (2015). Design of AC–DC PFC High-Order Converters with Regulated Output Current for Low-Power Applications. *IEEE Transactions on Power Electronics, Volume. 31*(3), 2012–2025. https://doi.org/10.1109/tpel.2015.2434937.

3. Boonraksa, P., Chaisa, A.T., et al. (March, 2022). Design and Simulation of Fuzzy logic controller based MPPT of PV module using MATLAB/ Simulink. *2022 International Electrical Engineering Congress (iEECON)*, 9-11. https://doi/ 10.1109/iEECON53204.2022.9741641.

4. Chowdhury, S., Kumar Das, D., & Hossain, M. S. (June, 2021), Power Performance Evaluation of a PV Module Using MPPT with Fuzzy Logic Control. *Journal of Engineering Advancements, Volume. 2*(1), 7-12. https://doi.org/10.38032/jea.2021.01.002.

5. Daud, A.K. & Khader, S. H. (2022). Closed Loop Modified SEPIC Converter for Photovoltaic System. *WSEAS Transaction on Circuits and Systems, Volume. 21*, 161-167. https://doi.org/ 10.37394/23201.2022.21.17.

6. Daud, A. K. & Khader, S. H. (2022). Comparison Analysis between Various Boost Chopper Configurations. *International Journal of Circuits and Electronics, Volume. 7*, 01-12. http://localhost:8080/xmlui/handle/123456789/8541.

7. Eltamaly, A. M. & Rezk, H. A. (2015). A comprehensive comparison of different MPPT techniques for photovoltaic systems. *Elsevier, Journal of Solar Energy, Volume. 112*, 1-12. https://doi.org/10.1016/j.solener.2014.11.010.

8. Femia, N., et al. (2005). Optimization of perturb and observe maximum power point tracking method. *IEEE Trans Power Electronics, Volume. 20* (4), 963–973. https://doi.org/10.1109/tpel.2005.850975.

9. Fernão, P. V., Foito, D., Baptista, F. & Fernando, S. J. (2016). Photovoltaic Generator System with A DC/DC Converter Based on An Integrated Boost-Ćuk Topology. *Elsevier, Solar Energy, Volume. 136*, 1–09. https://doi.org/10.1016/j.solener.2016.06.063.

10. Gilbert, M. M. (2017). *Renewable and Efficient Electric Power Systems. 2nd ed.* John Wiley & Sons, Inc. ch.4, 186-247. ISBN-13: 978-1118140628. http://www.a-ghadimi.com/files/Courses/Renewable%20Energy.

11. Hasan, J., Ferjana, S. & Chowdhury, S. (2021). Investigation of Power Performance of a PV Module with Boost Converter Using MATLAB Simulation. *American International Journal of Sciences and Engineering Research*, 01-13. https://doi.org/10.46545/aijser.v4i1.322.

12. Hanawa-Q Cell Specifications. (accessed 25 July, 2022). https://www.solaris-shop.com/hanwha-q-cells-q-peak-duo-blk-g5-315-315w-mono-solar-panel.

13. Hossain, Md. T., Rahman, Md. A. & Chowdhury, S. (Autumn, 2021). Evaluation of Power Performance of a PV Module with MPPT Solution Using MATLAB Simulation. *Journal of Renewable Energy and Environment, Volume. 8*(4), 101-107. https://www.jree.ir/article_137353_7bd16eed5df54abca03c789827fec020.pdf.

14. Khader, S. H. & Daud, A. K. (March, 2021). Boost chopper behaviors in Solar photovoltaic system. *Smart Grid and Renewable Energy,Volume. 12*(3), 31-52. https://doi.org/10.4236/sgre.2021.123003.

15. MATLAB and Simulink (2016) The MathWorks, Inc., version R2016b, http://www.mathworks.com.

16. Martini, S. S., Chebak, A. & Barka, N. (2015). Development of renewable energy laboratory based on integration of wind, solar and biodiesel energies through a virtual and physical environment. *3rd International Renewable and Sustainable Energy Conference, Marrakech*, 01-08. https://doi.org/10.1109/irsec.2015.7455086.

17. Mahmoud, Y., Xiao, W. & Zeineldin, H. H. (Jan, 2012). A simple approach to modeling and simulation of photovoltaic modules. *IEEE Trans. Sustain. Energy, volume. 3*(1), 185–186. https://doi.org/10.1109/tste.2011.2170776.

18. Mastromauro, R. A., Liserre, M. & Dell'Aquila, A. (May, 2012). Control issues in single-stage photovoltaic systems: MPPT, current and voltage control. *IEEE Trans. Ind. Information, volume. 8* (2), 241–254. https://doi.org/10.1109/tii.2012.2186973.

19. Mahdavi, M. & Farzanehfard, H. (Sept.,2011), Bridgeless SEPIC PFC Rectifier with Reduced Components and Conduction Losses. *IEEE Trans. Ind. Electronics, volume. 58* (9), 4253–4160, https://doi.org/10.1109/tie.2010.2095393.

20. Pavithra, K., Pooja, H., Tamilselvan, D. & Sudhakar, T. D. (2021). Solar power based positive output super-lift Luo converter using fuzzy logic controller. *Journal of Physics, Volume. 2040*, 01-12. https://doi.org/10.1088/1742-6596/2040/1/012034.

21. Robert, W. (May, 2022). The 10 best Solar Panels Manufacturers in the World, https://climatebiz.com/best-solar-panel-manufacturers/.

22. Solar-Log 2000, Palestine Polytechnic University. Industrial Synergy Center. (2022). https://isc.ppu.edu/en/campus/Productivity.

23. Solarex PV Specifications, (accessed 08 August, 2022) https://www.researchgate.net/figure/The-key-specifications-for-the-Solarex-MSX60-PV-panel-7_tbl2_283553910.

24. Solarex PV Specifications, (accessed 08 August, 2022). https://www.researchgate.net/figure/The-key-specifications-for-the-Solarex-MSX60-PV-panel-7_tbl2_283553910.

25. SUNPOWER Datasheet, SPR-315E-WHT-D. (accessed 25 July, 2022) http://www.solardesigntool.com/components/module-panel-solar/Sunpower/21/SPR-315E-WHT-D/specification-data-sheet.html.

26. Yatimi, H. & Aroudam, E. (2016). Assessment and control of a photovoltaic energy storage system based on the robust sliding mode MPPT controller. *Journal of Solar Energy, Volume. 139*. 557–568. https://doi.org/10.1016/j.solener.2016.10.038.

27. Zegaoui, A., Aillerie, M., Petit, P., Sawicki, J. P., Jaafar, A., Salame, C. & Charles, J. P. (2011). Comparison of two common maximum power point trackers by simulating of PV generators. *Energy Procedia, Volume. 6*, 678–687. https://doi.org/10.1016/j.egypro.2011.05.077.